Structural Determinants for the Membrane Interaction of Novel Bioactive Undecapeptides Derived from Gaegurin 5

Hyung-Sik Won,[†,||] Min-Duk Seo,[‡,||] Seo-Jeong Jung,[‡,⊥] Sang-Jae Lee,[§,#] Su-Jin Kang,[‡] Woo-Sung Son,[‡] Hyun-Jung Kim,[‡] Tae-Kyu Park,[†] Sung-Jean Park,[‡] and Bong-Jin Lee*[,‡,§]

[†]*Department of Biotechnology, Division of Life Sciences, College of Biomedical & Health Science, Konkuk University, Chungju, Chungbuk 380-701, Korea, National Research Laboratory (MPS), Research Institute of Pharmaceutical Sciences, College of Pharmacy, Seoul National University, Seoul 151-742, Korea, and Promeditech, Inc., Shilim-Dong 1578-51, Kwanak-Gu, Seoul 151-869, Korea*

Received October 6, 2005

Gaegurin 5 is a 24-residue, membrane-active antimicrobial peptide isolated from the skin of an Asian frog, *Rana rugosa*. We recently reported the antimicrobial activities of two novel undecapeptides derived from an inactive *N*-terminal fragment (residues 1−11) of gaegurin 5 (Won, et al. *J. Biol. Chem.* **2004**, *279*, 14784−14791). In the present work, the anticancer activities of the two antimicrobial undecapeptide analogues were additionally identified. The relationships between their structural properties and biological activities were assessed by characterizing the fundamental structural determinant for the basic membrane interaction. The circular dichroism and nuclear magnetic resonance results revealed that in a membrane-mimetic environment, the active peptides adopt a more stabilized helical conformation than that of the inactive fragment, and this conformation conferred an overall amphipathicity to the active peptides. Therefore, the most decisive factor responsible for the activity and selectivity could be the intramolecular amphipathic cooperativity, rather than the amphipathicity itself. Especially, the tryptophan residue of the active peptides seems to play a crucial role at the critical amphipathic interface that promotes and balances the amphipathic cooperativity by stabilizing both the hydrophilic and hydrophobic interactions with the membrane. Altogether, the present results suggest that the two novel undecapeptides are worthy of therapeutic development as new antibiotic and anticancer agents and provide structural information about their action mechanism.

Introduction

Membrane-active peptides exhibit many interesting biological and pharmacological activities, and particularly, membrane-active antimicrobial peptides are an important component of the innate defenses of all species of life.[1−9] Many antimicrobial peptides have little toxicity against animal cells, whereas they exhibit broad spectra of antimicrobial activity against diverse microorganisms, including drug-resistant bacteria. Accordingly, attention has been increasingly focused on antimicrobial peptides as potential therapeutic agents, and indeed, several antimicrobial peptides have been successful in pharmaceutical and commercial developments of new antibiotics.[8] In addition, some of the antimicrobial peptides and their analogues have been found to possess fungicidal, virucidal, and tumoricidal activities as well as bactericidal activity. Thus, new anticancer development using antimicrobial peptides has also been promoted recently.[9−12]

The skin of anurans (frogs and toads) has served as a rich source of bioactive peptides that can be subjected to therapeutic development.[8,13−16] Six antimicrobial peptides, named gaegurins (GGNs[a]), have been isolated from the skin of an Asian frog, *Rana rugosa*,[17−19] and some of them, particularly those with no or little hemolytic activity, are being considered as target molecules for the development of new antibiotic or anticancer agents.[20,21] GGNs belong to the best understood group of antimicrobial peptides, which is characterized by their cationic, amphipathic α-helical properties.[7,22] In membrane environments, the peptides adopt an amphipathic α-helical structure, whereas they assume a random-coil conformation in aqueous solutions. Therefore, the peptides are believed to function by the barrel-stave and/or carpet-like mechanism, leading to bacterial membrane disruption.[9,22−26] In the former mechanism, the transmembrane amphipathic α-helices form bundles, producing a transmembrane pore. The latter describes membrane disintegration by a disruption of the bilayer curvature, leading to micellization. In this model, in contrast to the barrel-stave mechanism, the peptides do not penetrate into the hydrophobic core of the membrane but rather bind to the phospholipid headgroups. For anticancer action, two general mechanisms have been suggested: cell necrosis via plasma membrane disruption or induction of apoptosis via mitochondrial membrane disruption.[9] In any case, the membrane-interacting ability is regarded as the most critical factor for both antimicrobial and anticancer activities of the peptides.

GGN5, a 24-residue antimicrobial peptide, is the shortest of the six GGNs and the one best characterized in terms of its 3D solution structure and structure−activity relationship.[27] In an effort to develop new, low molecular mass peptide antibiotics, we previously searched for the shortest GGN5 analogue peptide with favorable bioactivity by systematic peptide modifications

* To whom correspondence should be addressed. Phone: +8228807869. Fax: +8228723632. E-mail: lbj@nmr.snu.ac.kr.

[†] Konkuk University.

[‡] Seoul National University.

[§] Promeditech, Inc..

[||] These authors contributed equally to this work.

[⊥] Present address: Efficacy Research Department, National Institute of Toxicological Research, Korea Food & Drug Administration, Seoul 122-704, Korea.

[#] Present address: Structural Proteomics Laboratory, Department of Chemistry, College of Natural Sciences, Seoul National University, Seoul 151-742, Korea

[a] Abbreviations: CD, circular dichroism; DPC, dodecylphosphocholine; DQF-COSY, double-quantum filtered correlated spectroscopy; GGN, gaegurin; IC_{50}, concentration for 50% inhibition of cell growth; IC_{90}, concentration for 90% inhibition; NMR, nuclear magnetic resonance; NOE, nuclear Overhauser effect; NOESY, NOE spectroscopy; rmsd, root-mean-square deviation; SDS, sodium dodecyl sulfate; TOCSY, total correlation spectroscopy.

10.1021/jm050996u CCC: $33.50
Published on Web 07/08/2006

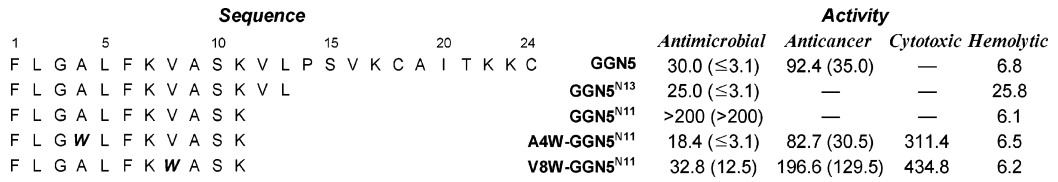

Figure 1. Comparison of the amino acid sequence and the biological activity between GGN5 and its analogues. Amino acid substitutions are indicated in bold faced, italicized letters. Antimicrobial activity is expressed by the average value (μg/mL) of the previously determined MICs against eight different bacteria, four Gram-positive (*B. subtilis*, *M. luteus*, *S. aureus*, and *S. epidermis*) and six Gram-negative bacteria (*E. coli*, *S. dysenteriae*, *S. typhimurium*, *K. pneumoniae*, *P. mirabilis*, and *P. aeruginosa*).[20] The lowest value of the eight MICs is presented in parentheses. For anticancer activity, the mean IC_{50} value against eight different tumor cell lines (A498, A549, HCT116, MCF-7, MKN45, NCl-H630, PC-3, and SK-OV-3) is presented, with the lowest IC_{50} in parentheses. Cytotoxic activity is provided by the IC_{50} value (μg/mL) against a normal breast cell line (MCF10a). Hemolytic activity is represented as % hemolysis at a 100 μg/mL peptide concentration against human erythrocytes, determined in the present study for the undecapeptides and determined previously for the others.[20]

Table 1. Antitumor Activities of Paclitaxel, GGN5, A4W-GGN5^{N11}, and V8W-GGN5^{N11}

	IC_{50}: μg/mL and (μM)				IC_{90}: μg/mL and (μM)			
cell line	paclitaxel	GGN5	A4W-GGN5^{N11}	V8W-GGN5^{N11}	paclitaxel	GGN5	A4W-GGN5^{N11}	V8W-GGN5^{N11}
A498	0.015	138.06	73.26	214.33	0.196	n.a.[a]	107.69	n.a.
	(0.017)	(54.1)	(56.5)	(169.1)	(0.229)		(83.18)	
A549	0.004	145.72	106.27	418.15	0.035	227.45	132.49	n.a.
	(0.0049)	(57.1)	(82.0)	(329.9)	(0.041)	(89.13)	(102.33)	
HCT116	0.002	113.31	30.48	144.37	0.007	227.45	72.81	215.08
	(0.0024)	(44.4)	(23.5)	(113.9)	(0.008)	(89.13)	(56.23)	(169.82)
MCF-7	0.002	183.74	77.29	198.87	0.013	238.17	141.96	290.14
	(0.0019)	(72.0)	(59.6)	(156.9)	(0.015)	(93.33)	(109.65)	(229.09)
MKN45	0.002	34.96	82.70	142.72	0.174	61.22	110.20	191.69
	(0.0026)	(13.7)	(63.8)	(112.6)	(0.204)	(23.99)	(85.11)	(151.36)
NCI-H630	0.021	41.85	75.92	129.54	0.317	64.10	105.24	148.80
	(0.024)	(16.4)	(58.6)	(102.2)	(0.372)	(25.12)	(81.28)	(117.49)
PC-3	0.015	43.64	123.81	174.15	0.710	58.46	145.27	246.95
	(0.017)	(17.1)	(95.5)	(137.4)	(0.832)	(22.91)	(112.20)	(194.98)
SK-MEL-2	0.006	47.47	30.48	n.a.[a]	0.032	46.44	60.56	n.a.
	(0.0072)	(18.6)	(23.5)		(0.037)	(18.20)	(46.77)	
SK-OV-3	0.004	38.28	92.15	150.45	0.060	59.82	115.39	210.19
	(0.0050)	(15.0)	(71.1)	(118.7)	(0.071)	(23.44)	(89.13)	(165.96)
MCF-10a			311.38	434.79			n.d.[b]	n.d.
			(240.5)	(343.4)				

[a] n.a.: not available; reproducible data could not be obtained even by three independent experiments. [b] n.d.: not detected; hardly reached 90% inhibition.

of both length and sequence.[20] We finally generated two synthetic peptide analogues of GGN5, namely, A4W-GGN5^{N11} and V8W-GGN5^{N11}, as property-optimized target molecules for new antibiotic development. These two undecapeptides are basically composed of the same amino acid sequence as the *N*-terminal 11-residue fragment of native GGN5 (namely, GGN5^{N11}), except for the fact that they possess a single amino acid substitution (tryptophan) at position 4 or 8 (Figure 1). Despite the fact that they are less than half the size of native GGN5, A4W-GGN5^{N11} and V8W-GGN5^{N11} showed bactericidal activities comparable to that of native GGN5 and depressed hemolytic activities in the range of that of GGN5. It is noteworthy, however, that GGN5^{N11} exhibited no biological activity, and GGN5^{N13} (*N*-terminal 13-residue fragment of GGN5) showed significant hemolytic activity as well as antimicrobial activity.

The present study sought to interpret the structure−activity relationships of A4W-GGN5^{N11} and V8W-GGN5^{N11}. We investigated the structural determinants of the peptides for membrane interaction, which is a critical process for their activity. Generally, the precise spectrum of bioactivity through membrane binding can be modified by a specific membrane interaction, depending on the lipid composition.[28−30] To identify the common, fundamental determinants for the basic interaction with the membrane, the 3D structures of these peptides were solved in an SDS micelle system, which is typically used as a simple membrane-mimetic environment.[20,21,31,32] Prior to structural elucidation, an extended examination of bioactivity is presented in this article. The present results provide useful information regarding the structure−activity relationships of the novel bioactive undecapeptides and will encourage advanced peptide engineering for the therapeutic development of new antimicrobial and anticancer peptides.

Results and Discussion

Bioactivity. We have previously documented the detailed spectrum of the antimicrobial activities of the undecapeptide analogues A4W-GGN5^{N11} and V8W-GGN5^{N11}. Many natural antimicrobial peptides are also known to exhibit anticancer activity.[9−12] Thus, in the present study, we examined the anticancer activities of the active undecapeptide analogues, although they were not originally designed to possess anticancer activity. Table 1 summarizes the IC_{50} and IC_{90} values against nine tumor cell lines from different tissues (also refer to Supporting Information, Figure 1). Experimental validation was performed by confirming that the IC_{50} values for the positive control agent, paclitaxel, agreed well with the literature values. As a result, the parent molecule GGN5 exhibited moderate anticancer activities, with IC_{50} values ranging from 18.98 to 99.57 μg/mL (13.7 to 72.0 μM) against various tumor cell lines. The active undecapeptide analogues of GGN5 also showed reasonable anticancer activities against the tumor cell lines: IC_{50} values ranging from 30.48 to 123.81 μg/mL (23.5 to 95.5 μM) for A4W-GGN5^{N11} and from 129.54 to 418.15 μg/mL (102.2

Table 2. Hemolytic Activities of GGN5N11, A4W-GGN5^{N11}, and V8W-GGN5^{N11} at Various Concentrations

peptide concn (ug/mL)	percent hemolysis values (%)		
	GGN5^{N11}	A4W-GGN5^{N11}	V8W-GGN5^{N11}
100	6.06	6.52	6.21
200	6.06	6.82	6.36
300	6.06	7.12	6.36
400	6.21	9.24	6.67

to 329.9 μM) for V8W-GGN5^{N11}. Although the anticancer activities of V8W-GGN5^{N11} were significantly weaker than those of GGN5, the anticancer activities of A4W-GGN5^{N11} were just slightly less than those of GGN5. In particular, the IC_{50} values of A4W-GGN5^{N11} against some tumor cell lines, such as A498, HCT116, MCF-7, and SK-MEL-2, were comparable to or lower than those of GGN5. These results suggest that the present antimicrobial peptide analogues are also noteworthy as potential compounds for the therapeutic development of an anticancer agent, by proper optimization through chemical modifications. In particular, considering their quite smaller size and comparable activity, the A4W-GGN5^{N11} and V8W-GGN5^{N11} peptides would be more useful than the native GGN5 as bioactive material. Thus, the cytotoxicity of the bioactive undecapeptides was further examined against normal human cells. The IC_{50} value of A4W-GGN5^{N11} against the normal, noncancerous breast cell line (MCF10a) was more than 4-fold higher than that against the breast tumor cell line, MCF-7 (Table 1). V8W-GGN5^{N11} also showed a more than 2-fold higher IC_{50} value against the normal cells than that against the tumor cells. In addition, neither peptide exhibited a significant increase in hemolytic activity, even at a much higher concentration than the IC_{90} values against most tumor cell lines (Table 2). Taken together, the present undecapeptide analogues, especially A4W-GGN5^{N11}, possess favorable activities for therapeutic development: high antimicrobial activity, moderate anticancer activity, and little cytotoxicity.

Much is known about the general mechanism by which antimicrobial peptides achieve their strong antimicrobial activities against microorganisms, with little cytotoxicity against normal human cells,[1−8] whereas less is known concerning their anticancer action mechanism. Generally, antimicrobial peptides function by disrupting cell membranes, and thus, the hydrophobic membrane interaction is the most critical factor for the activity. However, selective membrane permeation is achieved mainly by the positive charge of the peptides because the bacterial cell membrane surface is negatively charged, unlike the animal cell membrane surface, which is zwitterionic. Relating to this selective antimicrobial mechanism, the cancer cell membrane can be regarded as being similar to the bacterial membrane in that it has up to 8-fold more anionic phospholipids than do normal cell membranes.[12,33] On the basis of these insights, it could be reasonably assumed that the membrane-binding ability is the most critical factor for both the antimicrobial and anticancer activities. Thus, the structural properties of the bioactive peptides were characterized in detail as follows in relation to their membrane interactions.

Conformational Behavior. The native GGN5 peptide adopts a mainly unstructured, random-coil conformation in aqueous solution, whereas it folds into a functional conformation upon interaction with bacterial membranes.[20,27] The functional structure of GGN5 solved in SDS micelles[27] revealed an amphipathic α-helix conformation with a helical kink in the middle. The present three undecapeptide analogues of GGN5 exhibited distinct biological activities (Figure 1), despite their slight

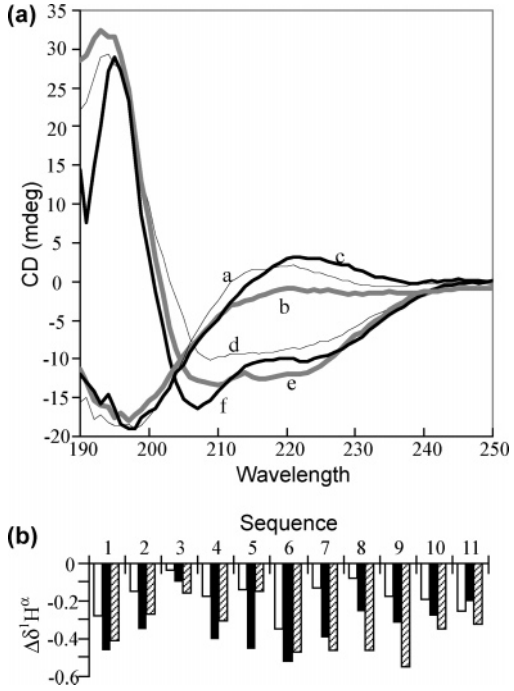

Figure 2. Comparison of helical propensity. (a) Far-UV CD spectra of GGN5^{N11} (a and d), A4W-GGN5^{N11} (b and e), and V8W-GGN5^{N11} (c and f), in water (a−c) and 10 mM SDS micelles (d−f). (b) $^1H^\alpha$ chemical shift deviations from random-coil values (GGN5^{N11}, white bars; A4W-GGN5^{N11}, black bars; V8W-GGN5^{N11}, striped bars). For the Gly residue, the average chemical shift values of the two detected $^1H^\alpha$ resonances were applied.

sequence variations.[20] These CD and NMR results implied that the helical propensities in a membrane-mimetic environment would be directly related to their biological activities. As revealed by the far-UV CD spectra in Figure 2a, the undecapeptide analogues of GGN5 (GGN5^{N11}, A4W-GGN5^{N11}, and V8W-GGN5^{N11}) have the same conformational preference as that of GGN5.[27] All of the undecapeptides were unstructured in water, as evidenced by the strong negative band near 198 nm and the positive band near 220 nm.[34,35] Only the most active peptide, A4W-GGN5^{N11}, showed slightly negative signals near 220 nm, alluding that the peptide would fold most easily into an ordered conformation in a membrane environment. Consistent with the CD spectra, the NMR spectra in water supported a disordered conformation of the three undecapeptides by showing a narrow dispersion of the backbone amide proton resonances and few interresidue NOEs (data not shown). In a widely used membrane-mimetic environment, SDS micelles,[20,21,31,32] the CD spectra indicated that all of the peptides adopted a helical conformation, as characterized by the strong negative bands from 208 to 222 nm and the strong positive band around 195 nm.[21,34] This conformational change from a random-coil in aqueous solution to an α-helix in membrane-mimetic environments is common to many membrane-binding peptides and, thus, supports the proposal that all three of the peptides would interact with biological membranes. However, the degree of conformational change, which could be correlated with the affinity to the membrane, is distinct between the inactive and active peptides. As judged from the signal intensities at 208 and 222 nm, the helical content of the inactive peptide GGN5^{N11} is much lower than that of the active peptides, A4W-GGN5^{N11} and V8W-GGN5^{N11}. In particular, the most active peptide, A4W-GGN5^{N11}, showed the highest signal intensity at 222 nm, where the helical content is most critically reflected.[27] In contrast, the moderately active peptide, V8W-GGN5^{N11}, exhibited a distinctly increased

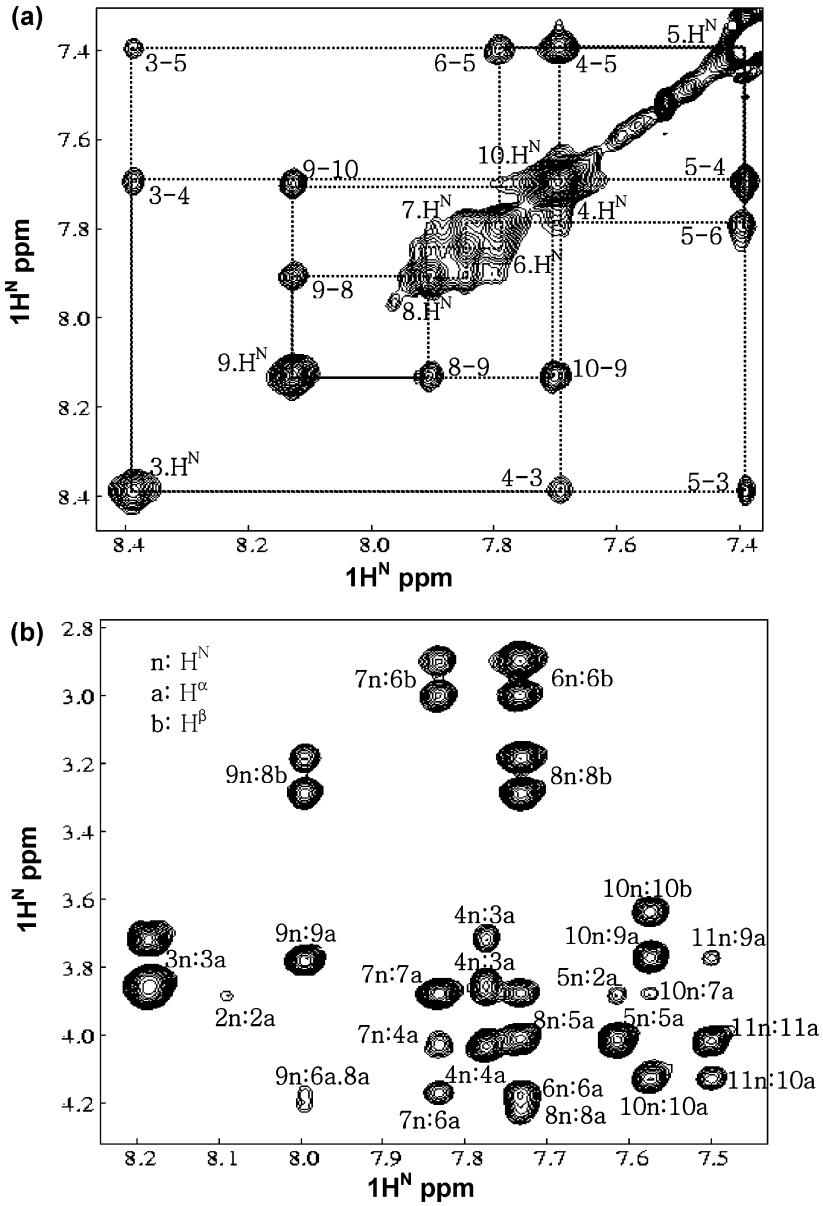

Figure 3. Selected region of the 2D NOESY spectra at a certain contour level. The amide (H^N-H^N correlation) region for A4W-GGN5^{N11} (a) and the fingerprint (H^N-H^α correlation) region for V8W-GGN5^{N11} (b) are shown. Each peak is labeled with its site-specific assignment, including the NOE correlation.

signal intensity at 208 nm, which suggests that the peptide includes a destabilized helix or flexible helical region. The results of the NMR chemical shift analysis in SDS micelles (Figure 2b) agreed well with the CD results. The negative $\Delta\delta^1H^\alpha$ (deviation of the $^1H^\alpha$ chemical shift from its random-coil value) indicated that all of the peptides possess helical propensity throughout the entire peptide region.[36] The active peptides, A4W-GGN5^{N11} and V8W-GGN5^{N11}, showed larger $\Delta\delta^1H^\alpha$ values than that of the inactive peptide, GGN5^{N11}. In particular, the $\Delta\delta^1H^\alpha$ intensification of the most active peptide, A4W-GGN5^{N11}, was larger in the *N*-terminal region than that of the moderately active peptide, V8W-GGN5^{N11}, whereas in the *C*-terminal region, V8W-GGN5^{N11} showed a larger $\Delta\delta^1H^\alpha$ intensification. In brief, the CD and NMR results indicated that the variations in biological activity originate from the differences in the helical contents or stability in membrane environments. A comparison between the A4W-GGN5^{N11} and V8W-GGN5^{N11} peptides suggests that *N*-terminal stabilization is particularly important for activity, which will be further discussed below.

Three-Dimensional Solution Structure. To elucidate the membrane-interacting features that are critical for both the antimicrobial and anticancer activities of A4W-GGN5^{N11} and V8W-GGN5^{N11}, more detailed information about the functional structure was obtained by determining their 3D NMR structures in an SDS micelle solution, as a membrane-mimetic environment.[27,32] Figure 3 shows the spectral dispersion and interresidue NOEs supporting the ordered structures of the peptides in SDS micelles. The NMR assignment results and the distance restraints for the structure calculation are provided as Supporting Information (Tables 1 and 2), and the structural statistics are presented in Table 3. Consistent with the CD and $\Delta\delta^1H^\alpha$ investigations (Figure 2), the ensemble structures of the three undecapeptides commonly showed helical conformations but differed in the helical length and stability (Figure 4). For the most active peptide, A4W-GGN5^{N11}, a stabilized α-helix element consisting of six or seven residues was observed in all of the individual molecules in the ensemble structure, and the α-helix of the energy-minimized average structure extended from Trp^4 to Ser^{10}.

Table 3. Structural Statistics of A4W-GGN5^{N11}, V8W-GGN5^{N11}, and GGN5^{N11}

	A4W-GGN5^{N11}	V8W-GGN5^{N11}	GGN5^{N11}
A. NMR restraints for structure calculation			
total distance restraints	105	77	67
intraresidual ($i = j$)	29	24	31
sequential ($\|i - j\| = 1$)	48	30	24
medium range ($1 < \|i - j\| < 5$)	28	23	12
B. ensemble statistics (20 conformers)			
violation analysis[a]			
average number of violations per molecule	0.5	1.2	0.6
average value of distance violation (Å)	0.10	0.06	0.06
maximum distance violation (Å)	0.24	0.22	0.21
energies (kcal/mol)[b]			
E_{total}	11.52 ± 0.07	11.52 ± 0.07	11.35 ± 0.07
E_{bonds}	0.053 ± 0.008	0.052 ± 0.004	0.047 ± 0.005
E_{angles}	11.18 ± 0.02	11.18 ± 0.01	11.03 ± 0.01
E_{NOE}	0.00005 ± 0.0001	0.00089 ± 0.0016	0.00094 ± 0.0017
$E_{impropers}$	0.117 ± 0.007	0.113 ± 0.007	0.110 ± 0.006
E_{vdw}	0.169 ± 0.052	0.175 ± 0.060	0.159 ± 0.059
rmsd (Å) to mean structure[c]			
backbone in α-helix region[d]	0.35 ± 0.12	0.49 ± 0.20	0.31 ± 0.15
all heavy atoms in α-helix region	1.16 ± 0.24	1.34 ± 0.30	1.57 ± 0.36
backbone in full region (residues 2−10)[e]	0.48 ± 0.15	0.90 ± 0.24	1.36 ± 0.34
all heavy atoms in full region	1.23 ± 0.24	1.63 ± 0.32	2.26 ± 0.39
Ramachandran plot analysis[f] (%)			
residues in most favored regions	89.4 (100)[g]	75.0 (87.5)	55.6 (50.0)
residues in additional allowed regions	10.6 (0)	23.1 (12.5)	38.8 (50.0)
residues in generously allowed regions	0 (0)	1.9 (0)	5.6 (0)
residues in disallowed regions	0 (0)	0 (0)	0 (0)

[a] Calculated by the AQUA program.[44] [b] Calculated in the CNS program.[43] [c] Calculated by the MOLMOL program.[45] [d] Residues 6−9 for GGN5^{N11}, 4−10 for A4W-GGN5^{N11}, and 5−10 for V8W-GGN5^{N11}. [e] The residues at termini were excluded. [f] Calculated by the PROCHECK program.[44] [g] The results for the energy-minimized average structure are presented in parentheses.

Furthermore, as judged from the rmsd value for the whole region (0.48 for the backbone; Table 3) of the ensemble structure (Figure 4), the helical loop conformation in the *N*-terminal region was rather well-ordered. In contrast, only a few molecules in the GGN5^{N11} ensemble structure contained either a short, 4-residue α-helix or a 3_{10}-helix, and its energy-minimized average structure showed a short α-helix from Phe^6 to Ala^9. In addition, the other regions were mainly disordered, yielding a rather high rmsd value for the whole region (Table 3). In the case of the moderately active peptide, V8W-GGN5^{N11}, α-helix elements in the ensemble structure were frequently found within the region from residues 4−10, which was similar to A4W-GGN5^{N11}. However, the helical length of V8W-GGN5^{N11} was generally shorter than that of A4W-GGN5^{N11}, and the α-helix in the energy-minimized average structure contained residues from Leu^5 to Ser^{10}. Additionally, a moderately ordered helical loop conformation was observed in the *N*-terminal region, which resulted in a moderately high rmsd value for the whole region (Table 3). From these inspections, it can be concluded that the tryptophan introduced in the active peptides contributed to inducing and stabilizing the helical conformation in their membrane-bound states, as supported by other examples showing the helix-stabilizing role of a tryptophan residue.[21,37] The results also indicate that GGN5^{N11} possesses a basic helical propensity, particularly in the region from Phe^6 to Ala^9 (Figure 4), which would afford a weak interaction with the membrane. Then, the substituted tryptophan in A4W-GGN5^{N11} and V8W-GGN5^{N11} could increase the membrane affinity of the peptides. Tryptophan is known as a representative membrane-interacting amino acid, and it often plays an important role by anchoring proteins to the lipid bilayer.[38,39] Finally, the tryptophan-induced membrane interaction would facilitate the adoption of a helical conformation, which is more favorable for the stabilized interaction. Accordingly, the biological activity, which is critically mediated by membrane interaction, exhibits a good correlation with the ability to adopt a helical conformation.

Structural Insight into the Membrane-Binding Mode. A detailed structural comparison between the present undecapeptides outlines why the helical adoption is more favorable for stabilized membrane binding, how tryptophan contributes to this stabilization, and what defines the decisive factor for activity. Basically, the amphipathic properties of the peptides could be a requirement for the amphiphilic interaction between the peptides and the membrane. In addition, the helical conformation effectively confers the amphipathic properties (Figure 5). Although all three of the undecapeptides might be *C*-terminally hydrophilic, because of their Lys^7, Ser^{10}, and Lys^{11} residues, the extended structures in the membrane-unbound state (modeled in Figure 5c) lack amphipathic characteristics because the side chain stretches are randomly directed and not immobilized. In contrast, as illustrated by the NMR structure (Figures 5a and b), the helical structures achieve amphipathic properties along the helical axis. When bound to the membrane (schematically modeled in Figure 5c), the amphipathic structure can contribute to both the hydrophilic interaction with the membrane surface and the hydrophobic interaction with the membrane interior. On the basis of this criterion, the inactive peptide (GGN5^{N11}) is just partially amphipathic and not immobilized, whereas the active peptides (A4W-GGN5^{N11} and V8W-GGN5^{N11}) possess overall amphipathicity that is relatively immobilized. Thus, the

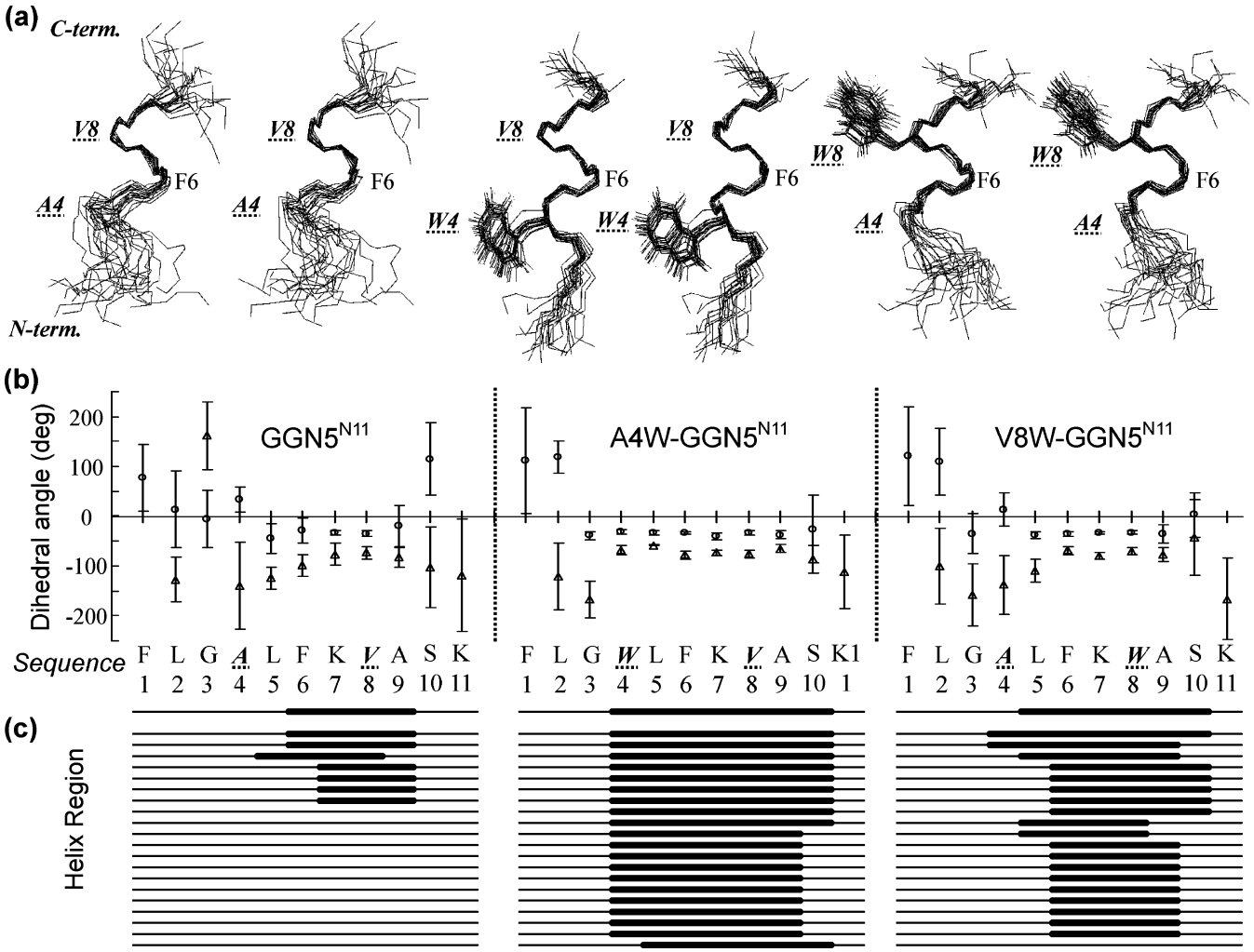

Figure 4. Backbone structures of GGN5^{N11} (left), A4W-GGN5^{N11} (middle), and V8W-GGN5^{N11} (right) in SDS micelles. (a) Stereo representations of the peptide backbones and the tryptophan side chains. The 20 structure ensembles were superimposed by matching the backbone atoms (N, Cα, and C′) in the structured α-helix region (residues 6−9 for GGN5^{N11}, 4−10 for A4W-GGN5^{N11}, and 5−10 for V8W-GGN5^{N11}). Sequence variations are indicated by the underlined bold faced, italicized letters. (b) Distributions of backbone dihedral angles. The average ϕ (△) and φ (○) angles with standard deviations (error bars) of the 20 structure ensembles are plotted along the sequences. (c) Location of the stabilized helix. The helix regions are indicated by thick lines along the sequence. The top lines are for the energy-minimized average structures (Figure 5) and the others are for the 20 structure ensembles.

structural amphipathicity, which is provided by the helical conformation, seems to be a critical requirement for biological activity.

Why do the two active peptides exhibit different degrees of activity? This question can be answered by a more detailed inspection of the amphipathic properties. As shown in Figure 5, the hydrophobic side chains in the inactive peptide are widely dispersed and scarcely contact each other, and the two lysines are not closely oriented. However, in the most active peptide (A4W-GGN5^{N11}), the hydrophobic side chains, including the tryptophan indole ring, converge into a hydrophobic cluster centered at the Leu^5 side chain, which is located and oriented in the direction exactly opposite to that of the lysine side chains. In other words, the hydrophobic side-chains, except for the flexible Phe^1, are oriented in close proximity, making frequent contacts with each other. This hydrophobic network is visualized by the frequent overlapping of the side chain surfaces in Figures 5a and c and is also supported by the NOESY spectra that contain interresidue NOEs between these side chain atoms (data not shown). In addition, because the helix in A4W-GGN5^{N11} is stabilized up to the *C*-terminus (Figure 4), the two lysine residues in the peptide are closer to each other than in the other peptides (Figure 5). In the structure of the moderately active peptide (V8W-GGN5^{N11}), both the hydrophobic and hydrophilic clusters are less compact than in the most active peptide (A4W-GGN5^{N11}) but are more converged than in the inactive peptide (GGN5^{N11}). Consequently, the most decisive factor for biological activity seems to be the intramolecular amphipathic cooperativity, rather than amphipathicity itself.

Finally, another critical factor determining the activity and selectivity is found in the location and orientation of the tryptophan residues in the active peptides. The only difference in the amino acid sequence between the inactive and active peptides is the tryptophan, which means that all of the structure−functional differences originated from this amino acid. In our previous examinations,[20] the peptide GGN5^{N13} (*N*-terminal 13-residue fragment of GGN5; Figure 1) showed significant hemolytic activity as well as high antimicrobial activity. Compared to GGN5^{N11}, GGN5^{N13} contains two more hydrophobic residues (Val^{12} and Leu^{13}) at the *C*-terminus, which would significantly contribute to the hydrophobic cooperativity but not to the hydrophilic cooperativity. In contrast, because of the single tryptophan residue, the hemolytic activity of A4W-GGN5^{N11} and V8W-GGN5^{N11} was effectively depressed, despite

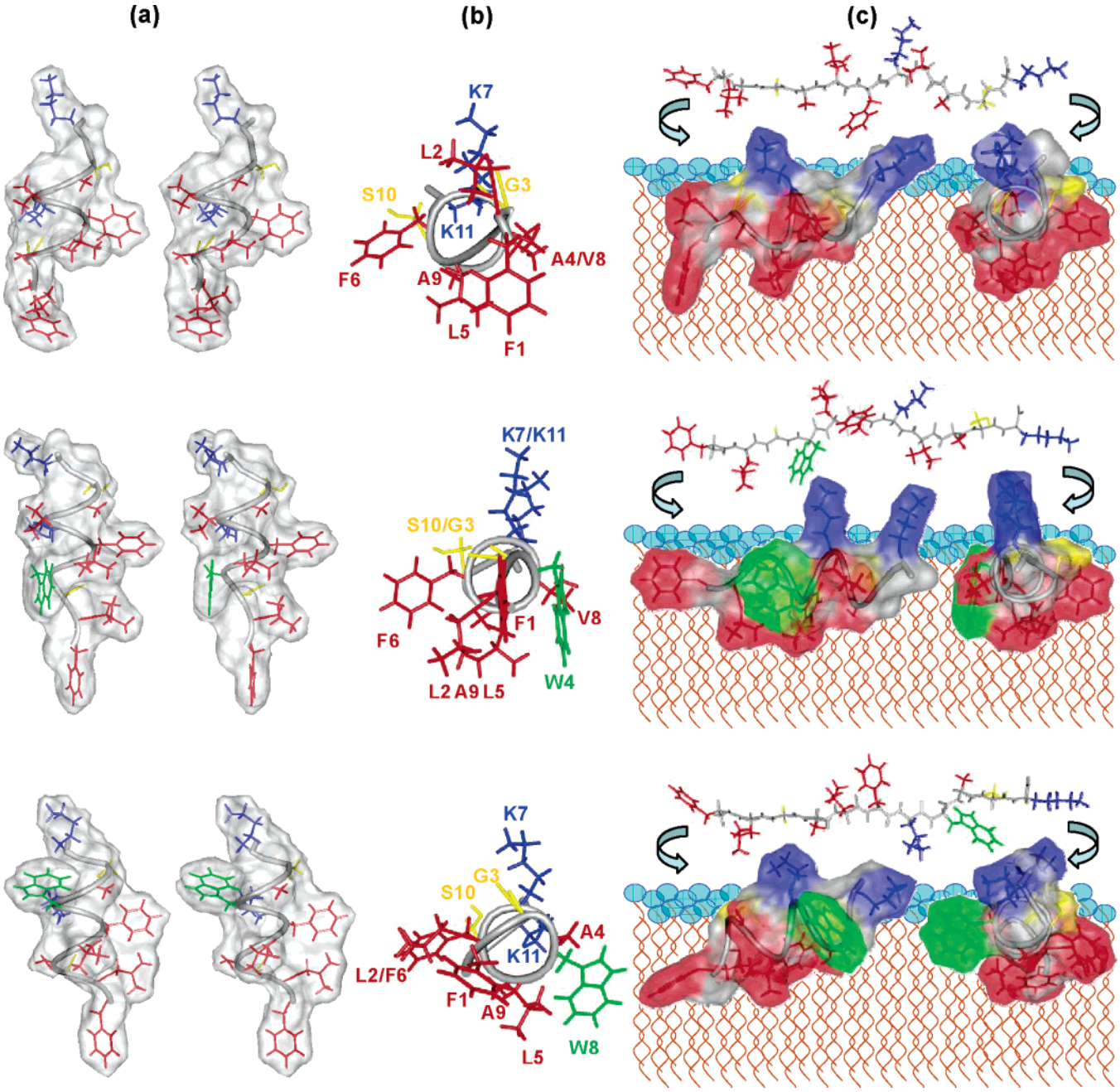

Figure 5. Amphipathic properties of GGN5^{N11} (top), A4W-GGN5^{N11} (middle), and V8W-GGN5^{N11} (bottom) in SDS micelles. The coordinates of the energy-minimized average structures were used for the drawing. Peptide backbones and side chains are illustrated as ribbon and stick presentations, respectively. The molecular surfaces are also presented in panels a and c. Colors are designated as follows: gray for backbone, blue for lysine (cationic, hydrophilic amino acid), yellow for glycine and serine (neutral and polar amino acids, respectively), green for tryptophan (amphiphilic amino acid), and red for the others (hydrophobic amino acids: alanine, valine, leucine, and phenylalanine). (a) Stereo representation of the structures. The viewpoint is approximately perpendicular to the helical axis. (b) Helical wheel diagram. The viewpoint is from the *N*-terminus to the *C*-terminus. (c) Schematic model of membrane binding. The surface colors are identical to the side chain colors.

high antimicrobial activity. This selective activity implies that tryptophan would contribute to both hydrophobic and hydrophilic interactions between the peptides and biological membranes. In both of the active undecapeptides, one interface between the hydrophobic side and the positively charged hydrophilic side (lysine residues) is occupied by the polar amino acid serine and the neutral amino acid glycine, whereas the other interface forms a critical boundary between the hydrophilic and hydrophobic sides (Figure 5b). The tryptophan residue is located at this critical amphipathic interface of the active peptides, and thus, it is reasonable to expect that tryptophan, in the membrane-bound peptide, would be positioned at the interface between the hydrophilic surface and the hydrophobic interior of the membrane (Figure 5c). It is noteworthy that tryptophan is highly amphiphilic in nature because its indole side chain is composed of a hydrophilic pyrrole ring and a hydrophobic benzene ring. As shown in Figure 5, the tryptophan indole side chains in the active peptides are positioned commonly in the direction opposite to the direction of the lysine stretches, and thus, the hydrophilic pyrrole ring and the hydrophobic benzene ring are oriented toward the hydrophilic and hydrophobic faces, respectively, of the peptides. This means that the indole side chain probably plays a dual role that contributes to the hydrophilic cooperativity by the pyrrole ring and the hydrophobic cooper-

ativity by the benzene ring. In addition, the tryptophan residues seem to play a regulatory role by balancing the hydrophobic and hydrophilic interactions. The amino acid sequence of the present undecapeptides is roughly characterized by the *N*-terminal region (up to Phe[6]), where hydrophobic amino acids are abundant, and the *C*-terminal region (from Lys[7]), where hydrophilic amino acids are predominant (extended structures in Figure 5c). Thus, the tryptophan position in A4W-GGN5^{N11} is closer to the hydrophobic residues than the hydrophilic residues, whereas the position in V8W-GGN5^{N11} is closer to the hydrophilic residues. As demonstrated in Figure 5, this results in the indole ring in A4W-GGN5^{N11} being flipped toward the hydrophobic core, which allows the benzene moiety to contribute to the hydrophobic network in a major fashion. In contrast, the indole ring in V8W-GGN5^{N11} is flipped over, which maximizes the hydrophilic interaction of the pyrrole ring. The minute variation in this tryptophanyl regulation seems to result in the slight difference in activity and selectivity between the A4W-GGN5^{N11} and V8W-GGN5^{N11} peptides.

Concluding Remarks. On the basis of our structural investigations, the structure−activity relationships of the bioactive undecapeptides can be summarized as follows. The antimicrobial and anticancer activities of the peptides probably correlate with their membrane-binding affinity. Although GGN5^{N11} has a basic propensity to assume an amphipathic helical conformation leading to membrane interaction, its membrane-binding affinity is not sufficient to yield biological activity and selectivity via selective membrane permeation because its amphipathicity and amphipathic cooperativity are not strong enough to stabilize membrane binding. However, the introduced tryptophan increases membrane-binding affinity so that the amphipathic helical structures of the membrane-bound peptides are more stabilized. Then, the tryptophan at the amphipathic interface strengthens the amphipathic interaction between the peptide and membrane by stabilizing both the hydrophilic interaction with the membrane surface and the hydrophobic interaction with the membrane interior. Consequently, the single amino acid substitution with tryptophan at position 4 or 8 loads both the activity and selectivity on the peptides. If the tryptophan position is more favorable for hydrophobic cooperativity than hydrophilic cooperativity, as at position 4 of A4W-GGN5^{N11}, then the activity enhancing effect becomes larger than the selectivity enhancing effect. If the position is more favorable for hydrophilic cooperativity, as at position 8 of V8W-GGN5^{N11}, then the activity enhancing effect becomes smaller, but the selectivity may be more significantly enhanced. With this regulation, the novel undecapeptide A4W-GGN5^{N11} could possess notable antimicrobial and anticancer activities with effectively depressed hemolytic activity.

Taken together, the present results suggest the powerful utility of the indole moiety at the amphipathic interface for antimicrobial and anticancer peptide engineering and the practical potential of the A4W-GGN5^{N11} peptide as a good lead molecule for the therapeutic development of new antimicrobial and/or anticancer agents. For this, it will be important to determine how the tryptophanyl contribution and the amphipathic cooperativity are specifically regulated, depending on the various lipid compositions of biological membranes.

Experimental Section

Materials and Peptide Preparation. Fmoc (9-fluorenylmethoxycarbonyl)-protected amino acids and Rink Resins were obtained from Advanced Chemtech, Inc. HPLC solvents were from Fisher Scientific. SDS-d_{25} was obtained from Isotec, and all other chemicals were of either analytical or biotechnological grade, obtained from various manufacturers. The chemically synthesized GGN5 (sequence: FLGALFKVASKVLPSVKCAITKKC) was purchased from ANYGEN (Kwang-ju, Korea; URL, http://www.anygen.com). The other peptides (GGN5^{N11}, A4W-GGN5^{N11}, and V8W-GGN5^{N11}; Figure 1) were synthesized by solid-phase methods using standard Fmoc chemistry, as described in detail previously.[20]

Anticancer and Hemolytic Assay. The anticancer activities of the present antimicrobial peptides were assessed from their cytotoxicity against nine tumor cell lines from different tissues: A498 (kidney), A549 (lung), HCT116 (colon), MCF-7 (breast), MKN45 (stomach), NCl-H630 (liver), PC-3 (prostate), SK-MEL-2 (skin), and SK-OV-3 (ovary). A normal breast cell line (MCF10a) was used as a negative control cell line, and a conventional drug (paclitaxel) was used as a positive control agent. The cytotoxicity assay was performed by the typical microculture MTT method.[27,40] Briefly, the cells were seeded at $0.25-0.5 \times 10^4$ cells/mL/well in 96 -well microtiter plates. The cells were then incubated at 37 °C overnight. When they were in the exponential growth phase, the drug was added. The cells in the wells were inoculated or not inoculated with the compounds dissolved in dimethyl sulfoxide. After a 3 day incubation with the drug, 50 μL of a 2 mg/mL solution of MTT reagent (in PBS at pH 7.0) was added to each well and incubated for 3 h. After removing the supernatant, 150 μL of dimethyl sulfoxide was added, followed by gentle shaking to dissolve the formazan crystals that remained in the wells. The absorbance was immediately recorded using a microplate reader at 570 nm. Wells without drugs were used for control cell viability, and wells without cells were used to blank the spectrophotometer. Cell growth inhibition was calculated by means of the formula % inhibition = (1-(absorbency of treated cells/absorbency of untreated cells)) $\times$ 100. IC_{50} and IC_{90} values for each cell line were evaluated at drug doses causing 50% and 90% absorbance reduction, respectively, in comparison to those of untreated control cells. Hemolytic activities of the undecapeptides were measured against human red blood cells, as described previously,[18,20,21,27] and were defined as % hemolysis values, compared to that by 0.2% Triton X-100.

Circular Dichroism. For CD spectroscopy, a precise amount of the peptide powder was dissolved to a final concentration of 50 μM in water and a 10 mM SDS solution, which is above its critical micellar concentration.[21,31,32] Far-UV CD spectra were obtained at 20 °C on a JASCO J-720 spectropolarimeter, using a 0.2 cm pathlength cell. CD scans were taken from 250 to 190 nm, with a 1 nm bandwidth, a 4 s response time, a scan speed of 50 nm/min, and a 0.2 nm step resolution. Three scans were added and averaged, followed by subtraction of the CD signal of the solvent.

NMR Spectroscopy and Structure Calculation. Samples for NMR measurements contained 3 mM peptide in a 300 mM SDS-d_{25} solution containing 7% D_2O at pH 4.0. Conventional 2D DQF-COSY, TOCSY (60 ms mixing time), and NOESY (80 and 150 ms mixing times) spectra were acquired by using a Bruker DRX-500 spectrometer at 313 K. The ^{1}H chemical shifts were referenced directly to the methyl signals of sodium 4,4-dimethyl-4-silapentane-1-sulfonate. The sequence-specific assignments of the proton resonances were achieved by spin system identification from the TOCSY and DQF-COSY spectra, followed by sequential assignments through the NOE connectivities.[20,21,41] Distance restraints were obtained mainly by manual assignments of the NOE cross-peaks in the NOESY spectra, and the CANDID module in the CYANA 2.0 program[42] was used to assign some ambiguous NOE cross-peaks. A total of 100 structures without any significant (>0.5 Å) violation were calculated for each peptide by the simulated annealing and energy minimization protocol in the program CNS 1.1.[43] Finally, 20 structures with the lowest energies and without distance violations over 0.3 Å were accepted for each peptide to represent ensemble structure and to obtain the energy-minimized average structure. The ensemble structures were validated by the PROCHECK and AQUA programs.[44] The rmsd values, secondary structure elements, and dihedral angles of the ensemble structures

were analyzed by the program MOLMOL.[45] The molecular graphics images in this article were produced by the UCSF Chimera program.[46]

Acknowledgment. This work was supported by the National R&D program for Cancer Control, Ministry of Health & Welfare (0420110-1), by the Ministry of Commerce, Industry and Energy through the Bio-Food and Drug Research Center at Konkuk University, Chungju, and in part by the National Research Laboratory Program (M10412000075-04J0000-03210) from the Korea Institute of Science & Technology Evaluation and Planning, Republic of Korea.

Supporting Information Available: NMR assignments, distance restraints used for the structure calculation, and the cytotoxicity assay. This material is available free of charge via the Internet at http://pubs.acs.org.

References

(1) Nicolas, P.; Mor, A. Peptides as Weapons against Microorganisms in the Chemical Defense System of Vertebrates. *Annu. Rev. Microbiol.* **1995**, *49*, 277−304.
(2) Gabay, J. E. Ubiquitous Natural Antibiotics. *Science* **1994**, *264*, 373−374.
(3) Hancock, R. E.; Scott, M. G. The Role of Antimicrobial Peptides in Animal Defenses. *Proc. Natl. Acad. Sci. U.S.A.* **2000**, *97*, 8856−8861.
(4) Yount, N. Y.; Yeaman, M. R. Immunocontinuum: Perspectives in Antimicrobial Peptide Mechanisms of Action and Resistance. *Protein Pept. Lett.* **2005**, *12*, 49−67.
(5) Yeaman, M. R.; Yount, N. Y. Mechanisms of Antimicrobial Peptide Action and Resistance. *Pharmacol. Rev.* **2003**, *55*, 27−55.
(6) Bechinger, B. Structure and Functions of Channel-Forming Peptides: Magainins, Cecropins, Melittin and Alamethicin. *J. Membr. Biol.* **1997**, *156*, 197−211.
(7) Dennison, S. R.; Wallace, J.; Harris, F.; Phoenix, D. A. Amphiphilic Alpha-Helical Antimicrobial Peptides and Their Structure/Function Relationships. *Protein Pept. Lett.* **2005**, *12*, 31−39.
(8) Zasloff, M. Antimicrobial Peptides of Multicellular Organisms. *Nature* **2002**, *415*, 389−395.
(9) Papo, N.; Shai, Y. Host Defense Peptides as New Weapons in Cancer Treatment. *Cell. Mol. Life Sci.* **2005**, *62*, 784−790.
(10) Kim, S.; Kim, S. S.; Bang, Y. J.; Kim, S. J.; Lee, B. J. In Vitro Activities of Native and Designed Peptide Antibiotics against Drug Sensitive and Resistant Tumor Cell Lines. *Peptides* **2003**, *24*, 945−953.
(11) Cruciani, R. A.; Barker, J. L.; Zasloff, M.; Chen, H. C.; Colamonici, O. Antibiotic Magainins Exert Cytolytic Activity against Transformed Cell Lines through Channel Formation. *Proc. Natl. Acad. Sci. U.S.A.* **1991**, *88*, 3792−3796.
(12) Rozek, T.; Wegener, K. L.; Bowie, J. H.; Olver, I. N.; Carver, J. A.; Wallace, J. C.; Tyler, M. J. The Antibiotic and Anticancer Active Aurein Peptides from the Australian Bell Frogs Litoria aurea and Litoria raniformis the Solution Structure of Aurein 1.2. *Eur. J. Biochem.* **2000**, *267*, 5330−5341.
(13) Won, H. S.; Kim, S. S.; Jung, S. J.; Son, W. S.; Lee, B.; Lee, B. J. Structure−Activity Relationships of Antimicrobial Peptides from the Skin of Rana esculenta Inhabiting in Korea. *Mol. Cells* **2004**, *17*, 469−476.
(14) Rinaldi, A. C. Antimicrobial Peptides from Amphibian Skin: An Expanding Scenario. *Curr. Opin. Chem. Biol.* **2002**, *6*, 799−804.
(15) Simmaco, M.; Mignogna, G.; Barra, D. Antimicrobial Peptides from Amphibian Skin: What Do They Tell Us? *Biopolymers* **1998**, *47*, 435−450.
(16) Barra, D.; Simmaco, M. Amphibian Skin: A Promising Resource for Antimicrobial Peptides. *Trends Biotechnol.* **1995**, *13*, 205−209.
(17) Park, J. M.; Jung, J. E.; Lee, B. J. Antimicrobial Peptides from the Skin of a Korean Frog, *Rana rugosa*. *Biochem. Biophys. Res. Commun.* **1994**, *205*, 948−954.
(18) Park, J. M.; Jung, J. E.; Lee, B. J. Antimicrobial Peptides from the Skin of a Korean Frog, *Rana rugosa*. *Biochem. Biophys. Res. Commun.* **1995**, *209*, 775.
(19) Park, J. M.; Lee, J. Y.; Moon, H. M.; Lee, B. J. Molecular Cloning of cDNAs Encoding Precursors of Frog Skin Antimicrobial Peptides from *Rana rugosa*. *Biochim. Biophys. Acta* **1995**, *1264*, 23−25.
(20) Won, H. S.; Jung, S. J.; Kim, H. E.; Seo, M. D.; Lee, B. J. Systematic Peptide Engineering and Structural Characterization to Search for the Shortest Antimicrobial Peptide Analogue of Gaegurin 5. *J. Biol. Chem.* **2004**, *279*, 14784−14791.
(21) Won, H. S.; Park, S. H.; Kim, H. E.; Hyun, B.; Kim, M.; Lee, B. J. Effects of a Tryptophanyl Substitution on the Structure and Antimicrobial Activity of C-Terminally Truncated Gaegurin 4. *Eur. J. Biochem.* **2002**, *269*, 4367−4374.
(22) Oren, Z.; Shai, Y. Mode of Action of Linear Amphipathic Alpha-Helical Antimicrobial Peptides. *Biopolymers* **1998**, *47*, 451−463.
(23) Shai, Y. Mode of Action of Membrane Active Antimicrobial Peptides. *Biopolymers* **2002**, *66*, 236−248.
(24) Hallock, K. J.; Lee, D. K.; Omnaas, J.; Mosberg, H. I.; Ramamoorthy, A. Membrane Composition Determines Pardaxin's Mechanism of Lipid Bilayer Disruption. *Biophys. J.* **2002**, *83*, 1004−1013.
(25) Porcelli, F.; Buck, B.; Lee, D. K.; Hallock, K. J.; Ramamoorthy, A.; Veglia, G. Structure and Orientation of Pardaxin Determined by NMR Experiments in Model Membranes. *J. Biol. Chem.* **2004**, *279*, 45815−45823.
(26) Hallock, K. J.; Lee, D. K.; Ramamoorthy, A. MSI-78, an Analogue of the Magainin Antimicrobial Peptides, Disrupts Lipid Bilayer Structure via Positive Curvature Strain. *Biophys. J.* **2003**, *84*, 3052−3060.
(27) Henzler-Wildman, K. A.; Lee, D. K.; Ramamoorthy, A. Mechanism of Lipid Bilayer Disruption by the Human Antimicrobial Peptide, LL-37. *Biochemistry* **2003**, *42*, 6545−6558.
(28) Henzler-Wildman, K. A.; Martinez, G. V.; Brown, M. F.; Ramamoorthy, A. Perturbation of the Hydrophobic Core of Lipid Bilayers by the Human Antimicrobial Peptide LL-37. *Biochemistry* **2004**, *43*, 8459−8469.
(29) Thennarasu, S.; Lee, D. K.; Tan, A.; Kari, P.; Ramamoorthy, A. Antimicrobial Activity and Membrane Selective Interactions of a Synthetic Lipopeptide MSI-843. *Biochim. Biophys. Acta* **2005**, *1711*, 49−58.
(30) Park, S. H.; Kim, H. E.; Kim, C. M.; Yun, H. J.; Choi, E. C.; Lee, B. J. Role of Proline, Cysteine and a Disulphide Bridge in the Structure and Activity of the Anti-Microbial Peptide Gaegurin 5. *Biochem. J.* **2002**, *368*, 171−182.
(31) Rodger, A.; Nord, B. *Circular Dichroism and Linear Dichroism*; Oxford University Press: New York, 1997.
(32) Won, H. S.; Lee, B. J. Nickel-Binding Properties of the C-Terminal Tail Peptide of *Bacillus pasteurii* UreE. *J. Biochem.* **2004**, *136*, 635−641.
(33) Stafford, R. E.; Fanni, T.; Dennis, E. A. Interfacial Properties and Critical Micelle Concentration of Lysophospholipids. *Biochemistry* **1989**, *28*, 5113−5120.
(34) Buchko, G. W.; Rozek, A.; Hoyt, D. W.; Cushley, R. J.; Kennedy, M. A. The Use of Sodium Dodecyl Sulfate to Model the Apolipoprotein Environment. Evidence for Peptide-SDS Complexes Using Pulsed-Field-Gradient NMR Spectroscopy. *Biochim. Biophys. Acta* **1998**, *1392*, 101−108.
(35) Wishart, D. S.; Sykes, B. D.; Richards, F. M. The Chemical Shift Index: A Fast and Simple Method for the Assignment of Protein Secondary Structure through NMR Spectroscopy. *Biochemistry* **1992**, *31*, 1647−1651.
(36) Scudiero, D. A.; Shoemaker, R. H.; Paull, K. D.; Monks, A.; Tierney, S.; Nofziger, T. H.; Currens, M. J.; Seniff, D.; Boyd, M. R. Evaluation of a Soluble Tetrazolium/Formazan Assay for Cell Growth and Drug Sensitivity in Culture Using Human and Other Tumor Cell Lines. *Cancer Res.* **1988**, *48*, 4827−4833.
(37) Utsugi, T.; Schroit, A. J.; Connor, J.; Bucana, C. D.; Fidler, I. J. Elevated Expression of Phosphatidylserine in the Outer Membrane Leaflet of Human Tumor Cells and Recognition by Activated Human Blood Monocytes. *Cancer Res.* **1991**, *51*, 3062−3066.
(38) Park, K.; Oh, D.; Shin, S. Y.; Hahm, K. S.; Kim, Y. Structural Studies of Porcine Myeloid Antibacterial Peptide Pmap-23 and Its Analogues in Dpc Micelles by NMR Spectroscopy. *Biochem. Biophys. Res. Commun.* **2002**, *290*, 204−212.
(39) Hu, W.; Lee, K. C.; Cross, T. A. Tryptophans in Membrane Proteins: Indole Ring Orientations and Functional Implications in the Gramicidin Channel. *Biochemistry* **1993**, *32*, 7035−7047.
(40) Ridder, A. N.; Morein, S.; Stam, J. G.; Kuhn, A.; de Kruijff, B.; Killian, J. A. Analysis of the Role of Interfacial Tryptophan Residues in Controlling the Topology of Membrane Proteins. *Biochemistry* **2000**, *39*, 6521−6528.
(41) Wüthrich, K. *NMR of Proteins and Nucleic Acids*; Wiley: New York, 1986.
(42) Herrmann, T.; Guntert, P.; Wüthrich, K. Protein NMR Structure Determination with Automated Noe Assignment Using the New Software Candid and the Torsion Angle Dynamics Algorithm Dyana. *J. Mol. Biol.* **2002**, *319*, 209−227.
(43) Brunger, A. T.; Adams, P. D.; Clore, G. M.; DeLano, W. L.; Gros, P.; Grosse-Kunstleve, R. W.; Jiang, J. S.; Kuszewski, J.; Nilges, M.; Pannu, N. S.; Read, R. J.; Rice, L. M.; Simonson, T.; Warren, G. L. Crystallography & NMR System: A New Software Suite for Macromolecular Structure Determination. *Acta Crystallogr., Sect. D* **1998**, *54*, 905−921.

(44) Laskowski, R. A.; Rullmann, J. A.; MacArthur, M. W.; Kaptein, R.; Thornton, J. M. Aqua and Procheck-NMR: Programs for Checking the Quality of Protein Structures Solved by NMR. *J. Biomol. NMR* **1996**, *8*, 477−486.
(45) Koradi, R.; Billeter, M.; Wüthrich, K. Molmol: A Program for Display and Analysis of Macromolecular Structures. *J. Mol. Graph.* **1996**, *14*, 51−5, 29−32.
(46) Pettersen, E. F.; Goddard, T. D.; Huang, C. C.; Couch, G. S.; Greenblatt, D. M.; Meng, E. C.; Ferrin, T. E. UCSF Chimera−a Visualization System for Exploratory Research and Analysis. *J. Comput. Chem.* **2004**, *25*, 1605−1612.

JM050996U